Dynamics and Ordering in a Spin-Labeled Oligonucleotide Observed by 220 GHz Electron Paramagnetic Resonance

David E. Budil,* Stephen V. Kolaczkowski,* Alex Perry,‡ Chamakura Varaprasad,‡ Francis Johnson,‡ and Phyllis R. Strauss†

Departments of *Chemistry and †Biology, Northeastern University, Boston, Massachusetts 02115; and ‡Department of Pharmacological Sciences, State University of New York at Stonybrook, Stonybrook, New York 11794 USA

ABSTRACT The dynamics of a newly synthesized cytosine spin-label and the spin-labeled pentamer TTC*TT have been observed by high-frequency (220 GHz) electron paramagnetic resonance (EPR) in aqueous solution at ambient temperature using only nanomolar amounts of spin-label. Temperature studies were carried out for both labeled species in buffer containing glycerol. The motion of the spin-labeled monomer could be fitted using a model of fully anisotropic rotation (FAR) over the entire temperature range studied. In the single-stranded pentamer, the high-field spectra are best interpreted using a model of microscopic ordering with macroscopic disorder (MOMD) with the probe in a highly nonpolar environment. The observed local order parameters of 0.60–0.70 suggest a micelle-like structure in which the label is tightly packed with the hydrophobic bases. These preliminary studies illustrate how the excellent orientation selectivity of high-field EPR provides new dynamic information about local base motions in DNA, and also how high-field EPR of spin-labels allows one to discriminate accurately between the effects of local versus global motions in spin-labeled macromolecules.

INTRODUCTION

Elucidating the detailed motional dynamics of DNA is of central importance in many areas of chemistry, biochemistry, and biotechnology. Electron paramagnetic resonance (EPR) of macromolecules specifically labeled with a stable nitroxide has been demonstrated to be an excellent probe for position-dependent dynamics in oligonucleotides (Bobst et al., 1996; Keyes et al., 1997; Kao and Bobst, 1985; Pauly et al., 1987; Strobel et al., 1990; Keyes and Bobst, 1995; Spaltenstein et al., 1988, 1989; Hustedt et al., 1993, 1995) as well as in site-specifically labeled peptides and proteins (Berliner and Reuben, 1989; Likhtenshtein, 1993; Millhauser, 1992; Altenbach and Hubbell, 1994).

Although EPR has provided considerable insight into both the global and local dynamics of DNA molecules, substantially different results have been reported for different types of spin-labels, and some important aspects of the problem remain unresolved. There have been two major approaches to covalent labeling of DNA. Bobst and coworkers (Bobst et al., 1996; Keyes et al., 1997; Kao and Bobst, 1985; Pauly et al., 1987; Strobel et al., 1990; Keyes and Bobst, 1995) have utilized flexible tethers of 2–5 atoms and applied two models, the "dynamic cylinder" and "base disk" models (Keyes and Bobst, 1995) in order to separate the effects of internal and overall dynamics. In the dynamic cylinder model, the spin probe motion is characterized in terms of a local order parameter S, which depends on tether length and reflects the local dynamics. In the base-disk model, the base disk correlation time, $\tau_\perp$, is sensitive both to local base dynamics and to the overall motion of the DNA, but comparison of the two models leads to the relation $\tau_\perp \propto S^2\tau_{rb}$, where τ_{rb} is the correlation time for the rigid-body rotation of the DNA molecule.

In a different approach, Robinson and co-workers (Spaltenstein et al., 1988; Spaltenstein et al., 1988; Hustedt et al., 1993, 1995) have utilized rigid 2- and 4-atom acetylenic linkages in order to restrict the degrees of freedom of local label motion and probe the base motion more directly. The spectra of an acetylene-tethered nitroxide incorporated into oligomers of various lengths showed significant dependence on the size of the DNA, suggesting that they mainly reflected bending and global tumbling motions of the DNA itself. Collective bending motions, as well as individual base and spin-label motions, were accounted for by using effective averaged g and A tensors. These workers have concluded that the spin-label motion consists mainly of uniaxial rotation about the acetylene-tether bond(s) with very little DNA base motion, in contrast to the results obtained using more flexibly attached labels. However, it has been suggested based on evidence from melting curve studies (Froehler et al., 1992) that the rigid acetylenic tether itself may act to restrict base motion by increasing base stacking. The precise relationship between base-stacking energy and local dynamics remains unclear.

An alternative to resolving the combined effects of base and probe motion is to study the spin-label over a range of EPR frequencies, including very high frequencies. At the conventional EPR frequency of 9 GHz, the spectra are affected by the slower bending and tumbling motions of the DNA as well as by the more rapid internal spin label motion. These combined effects lead to the ambiguities noted above in resolving the details of the local spin-label motion at 9 GHz. In contrast, at frequencies above 150 GHz,

Received for publication 4 March 1999 and in final form 20 October 1999.

Address reprint requests to Dr. David E. Budil, Dept. of Chemistry, Northeastern University, 102 Hurtig Hall, 360 Huntington Ave., Boston, MA 02115. Tel.: 617-373-2369; Fax: 617-373-8795; E-mail: dbudil@neu.edu.

0006-3495/00/01/430/09 $2.00

slower macromolecular motions are effectively "frozen out," and the spectra are most sensitive to the fast time scales that typify local label dynamics. High-frequency EPR thus provides a direct spectroscopic means to resolve the dynamic effects of large-scale versus local probe motion.

In addition, the increased orientation resolution for nitroxides at higher frequencies provides much greater sensitivity to details of the dynamics such as rotational anisotropy (Budil et al., 1993) and local ordering of the label. For example, at high field it is frequently possible to determine ordering parameters for more than one axis by measuring higher-order terms in the local orienting potential. Resolution of rotational correlation times around individual axes of the probe molecule may also identify the particular axis for which the motion is most sensitive to such effects as local base motion, conformational changes, and DNA size.

Until recently, it had been difficult to obtain EPR spectra of aqueous samples at millimeter wavelengths because of the significant dielectric losses caused by water at these wavelengths. These difficulties have now been overcome (Barnes and Freed, 1997; Cardin et al., 1999) making it possible to study spin-labeled DNA in aqueous buffers and at physiological temperatures. One of the initial objectives of this work was therefore to establish that 220 GHz EPR may be applied to study spin-labeled DNA with sufficient concentration sensitivity to enable accurate analysis of the motion. For this preliminary study we have selected a short oligonucleotide (specifically a single-stranded pentamer) labeled with a newly synthesized cytidine analog (Fig. 1 *a, inset*).

We find the high-frequency spectra are indeed quite sensitive to the local motional anisotropy of the probe, and also permit characterization of local probe ordering in the labeled pentamer. The results illustrate the significant advantages that high-frequency EPR offers for studying the details of spin-labeled biopolymers in aqueous media at physiological temperatures.

EXPERIMENTAL

Synthesis of spin-label

The spin-label plus tether [2,2,6,6-tetramethyl-4-(2-aminoethyl) piperidone1-oxyl] was synthesized from commercially available 2,2,6,6-tetramethylpiperidone-4-monohydrate in three steps: 1) oxidation of the starting material by sodium tungstate in the presence of hydrogen peroxide (MeOH-CH_3CN 12:1, RT, 48 h) followed by 2) reductive amination (N-acetyl ethylene diamine hydrochloride, $NaCNBH_3$, MeOH, RT, 48 h) and 3) hydrolysis by NaOH (EtOH-H_2O 1:1, reflux, 40 h).

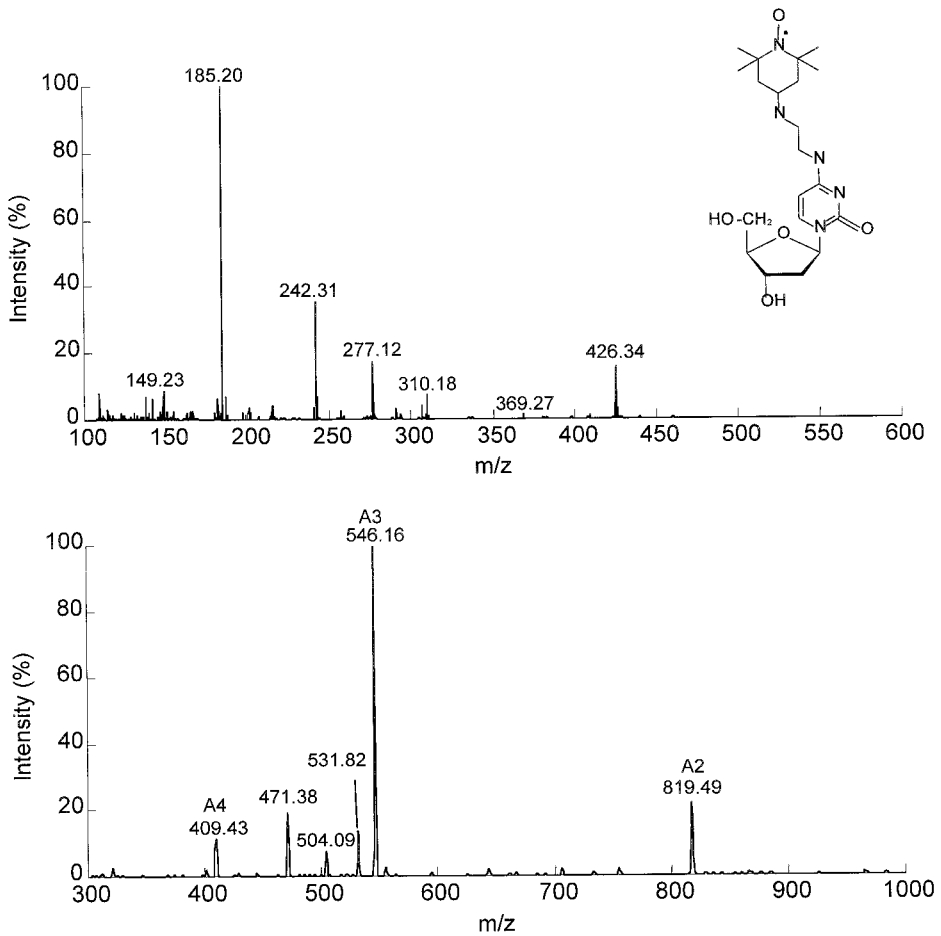

FIGURE 1 Mass spectra of (*a*) cytosine-analog spin-label TAPDC and (*b*) the pentamer TTC*TT incorporating the label, obtained under experimental conditions described in the text. The peaks marked A2, A3, and A4 identify the charge ladder for multiple ionizations of the pentamer, for which the singly ionized species corresponds to 1641.5. No peaks were observed above the *m/z* range shown. The *inset* shows the structure of TAPDC.

Synthesis of labeled cytosine

The spin-label was reacted with 3′,5′-O-*bis*-tert-butyldimethylsilyl-N^4-triazolo-2′deoxyuridine (Reese and Skone, 1984) in dichloromethane for 24 h at RT, and the silyl groups were subsequently cleaved using tetrabutylammonium fluoride (2.8 equivalents, 0.1 M in THF, 24 h at RT in dichloromethane) to afford the labeled nucleoside, N^4-[2,2,6,6-tetramethyl-4-(2-aminoethyl)-piperidin-1-oxyl]-2′-deoxycytosine (TAPDC) shown in Fig. 1.

Synthesis of labeled pentamer

The labeled pentamer was obtained with a post-polymerization modification of DNA. Commercially available thymidine phosphoramidite and convertible nucleoside (N^4-triazolo-dU, obtained from Glen Research Corp., Sterling, VA) were used to synthesize the oligomer 5′-DMT-TTXTT-Resin (where X = N^4-triazolo-dU) on a DNA synthesizer (Applied Biosystems, Foster City, CA). The triazolo group on the pentamer was substituted with the spin-label amine (0.1 M, CH_3CN, 2 h, RT > 90% conversion), and the DNA was released from the resin with conc. NH_4OH. The DMT-pentamer was purified by reverse-phase HPLC eluted with triethyl ammonium acetate, 0.1 M, pH 7.1, followed by CH_3CN. The major peak from the preparative HPLC was collected and hydrolyzed with 80% aqueous acetic acid to give the final product, the pentamer 5′-TTC*TT-3′, where C* indicates the labeled cytidine residue.

Characterization

The final products were purified by reversed-phase HPLC on a C18 column by elution with a mixture of (A) 0.1 M triethyl ammonium acetate buffer, pH 7.1, and (B) CH_3CN, with a gradient from 95% A to 80% A. Both the monomer and the labeled pentamer were further characterized by mass spectroscopy as described below.

Mass spectra of the labeled cytosine were obtained on a Micromass Trio 2000 instrument using a glycerin matrix and fast atom bombardment with xenon gas at 7 kV and 1 mA of ion current. Scans were obtained in positive ion mode from m/z = 100-1000 in 3 s. The MH^+ ion appeared at mass-to-charge (m/z) ratio of 426.3 ± 0.3 as shown in Fig. 1 *a*.

Electrospray ionization mass spectroscopy of the pentamer was performed on a Quattro LC (Micromass, UK). Infusion experiments were carried out with the sample diluted to ~1 μM in 50% CH_3CN/H_2O. A syringe pump (Harvard Apparatus, Holliston, MA) supplied a constant flow of 50% CH_3CN/H_2O at 5 mL/min. The instrument was operated in the negative ion mode with the probe voltage set to −3.2 kV and the cone voltage set to −31 V. The source temperature was 100°C and the desolvation temperature was 150°C. Nitrogen was used as both the drying and nebulization gas at 10 L/min and 1.4 L/min, respectively. The mass range m/z 300-1600 was scanned in 5 s averaging several scans for each spectrum. Fig. 1 *b* shows the mass spectrum of the labeled pentamer in the range m/z = 300-1000. The spectrum exhibits a "charge ladder" of peaks at m/z = 409.43, 546.16, and 819.49, corresponding to the species $(M-nH)^{n-}$ for n = 2, 3, and 4, respectively. This series corresponds to a singly ionized species with m/z = 1641.5 ± 0.3. Under the experimental conditions given, no peaks were observed above m/z = 1000.

The near-exact agreement of the m/z values of the parent ions with the predicted values of 424.5 for TAPDC and 1641.3 for 5′-TTC*TT-3′, confirms the identities of the both the monomer label and the labeled pentamer. No major impurity was found in the mass spectra of either compound, although minor unassigned peaks in the EIS-MS of the pentamer were observed as shown in Fig. 1 *b*.

220 GHz EPR spectroscopy

A detailed description of the locally constructed 220 EPR GHz spectrometer has been given elsewhere (Cardin et al., 1999). Samples were placed in a thin (15–20 μm) aqueous layer held between two 160–170-μm-thick quartz coverslips (ESCO Products, Oak Ridge, NJ) similar to those described by Barnes and Freed (1997). The sample concentrations ranged from 700 μM to 4.3 mM in spin-label, as noted below and in the figure captions. The labeled nucleotide and oligonucleotide were both dissolved in 50 mM HEPES buffer at pH 7.4. The volume of sample in the active area of the sample cell was ~300 nL, although 3 μL was typically used to fill the cell. Spectra were obtained using standard field-modulation methods with a modulation amplitude of 1.5 G or less at 100 kHz.

RESULTS AND DISCUSSION

Single-scan spectra of 4.3 mM labeled monomer in aqueous solution at 18°C and in 75% glycerol at temperatures between 0°C and 18°C are shown in Fig. 2. An analogous set of spectra obtained from the labeled pentamer, 3.5 mM in aqueous solution and in 35% glycerol at temperatures between 18°C and −31°C is shown in Fig. 3. The spectrum obtained in the near-rigid limit (at the lowest temperature shown in Fig. 3) was used to determine the g and A tensors of the probe, which are summarized in Table 1.

Because of the much larger linewidths observed in the slow-motion regime at 220 GHz, higher concentrations are required in order to obtain a signal-to-noise ratio that allows accurate lineshape analysis. The spin-label concentrations used for 220 GHz spectroscopy are therefore substantially higher than those that have typically been used at X-band. Care was taken to verify that the lineshapes were not concentration-dependent for the labeled species studied. Despite the requirement of the present instrumentation for higher concentrations, however, the sensitivity of the high-field spectrometer still compares quite well with spectrometers at conventional frequencies: because of the very small sample volume utilized in our sample cavity, the spectra shown in Figs. 2 and 3 required only 0.21–1.30 nmol of DNA per sample.

Analysis of monomer label in fast-motion limit

The spectrum obtained from the monomer in aqueous solution (Fig. 2, *top spectrum*) exhibits the three-line pattern characteristic of a nitroxide in the fast-motion regime. The homogeneous widths of the three lines may be expressed as

$$T_2^{-1}(M_I) = A + BM_I + CM_I^2 \qquad (1)$$

where M_I identifies the nuclear state of each ^{14}N hyperfine line. The A/B and C/B ratios measured at high frequency, together with the magnetic parameters, can be used to obtain two linear "allowed-value" equations (Budil et al., 1993; Kowert, 1981) which fully determine the rotational anisotropy of the probe. Specifically, one obtains the anisotropy parameters $\rho_x = R_x/R_z$ and $\rho_y = R_y/R_z$, where R_x, R_y, and R_z are the rotational diffusion rate constants around each axis of the spin probe.

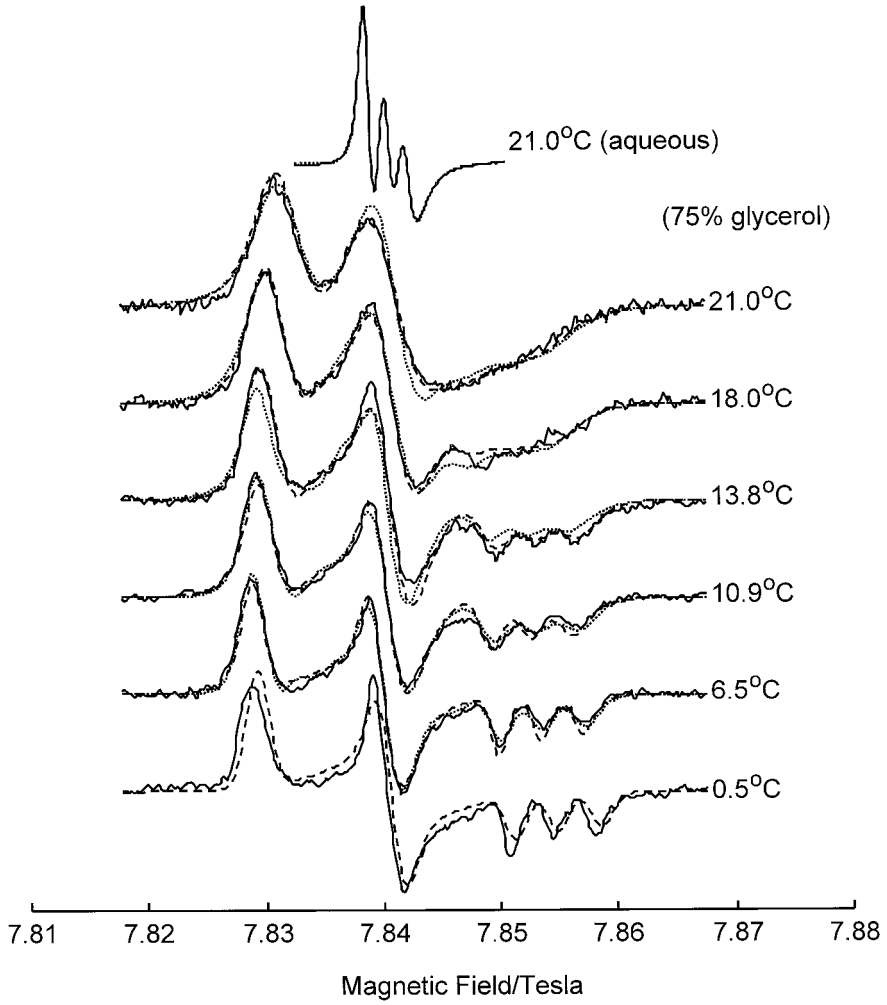

FIGURE 2 220 GHz EPR spectra of 4.2 mM cytosine spin-label in HEPES buffer at 21°C (*top spectrum*) and in buffer with 75% (by volume) glycerol as a function of temperature. Dashed lines show the least-squares fits obtained for the FAR model as described in the text. Dotted lines for spectra at 21.0°C, 18.0°C, and 13.8°C show the spectrum calculated assuming an axially symmetric diffusion tensor as described in the text.

The peaks in the fast-motion spectrum at 220 GHz are well represented by the simple Lorentzian lineshape, since the inhomogeneous linewidth is much smaller than the homogeneous linewidth due to spin relaxation at the higher fields. The *A*, *B*, and *C* parameters were therefore calculated directly from the linewidths obtained by fitting three Lorentzian lines to each spectrum. The excellent signal-to-noise ratios of the spectra also allowed a reasonably accurate measurement of the small *C* parameter, so that both the *A*/*B* and the *C*/*B* ratios could be determined at 220 GHz. The measured ratios were $A/B = 5.65 \pm 0.07$ and $C/B = 0.039 \pm 0.006$, based on the average of fittings to five spectra. Solution of the *A*/*B* and *C*/*B* allowed-value equations (Budil et al., 1993) yielded the rotational anisotropy parameters $\rho_x = 5.0 \pm 0.7$ and $\rho_y = 1.3 \pm 0.5$.

The fast-motional results clearly indicate that the axis of fastest rotation of the spin-label is closest to the *x* axis of the nitroxide, which is the N—O bond direction. Although this simplified treatment neglects the possibility that the diffusion axes may be tilted away from the magnetic axes, the results are quite consistent with the expected rapid rotation of the probe molecule around its tether.

Analysis of labeled monomer and pentamer in slow-motion regime

The spectrum from the labeled pentamer in aqueous solution at 21°C is significantly slower than that from the monomer under the same conditions. The spectrum of a 700 μM sample in aqueous buffer (Fig. 3, *top*) consists of a single broad and relatively featureless peak, indicating dynamics in the incipient slow-motion regime at 220 GHz. The rotational anisotropy and/or local ordering parameter of the probe could not be uniquely determined from the spectrum under these conditions.

More complete details of the local probe dynamics may be obtained when the rotational rates fall into the slow-motional regime for a given EPR frequency. At 220 GHz, it was necessary to reduce the rotational rate by increasing the viscosity of the buffer with added glycerol, for both the monomer and pentamer. Approximately 75% (by volume) glycerol was required to bring the monomer rotation into the slow-motional regime at room temperature. Significantly less glycerol (35%) was needed for the pentamer, given that it exhibited motional rates at least five times slower than the

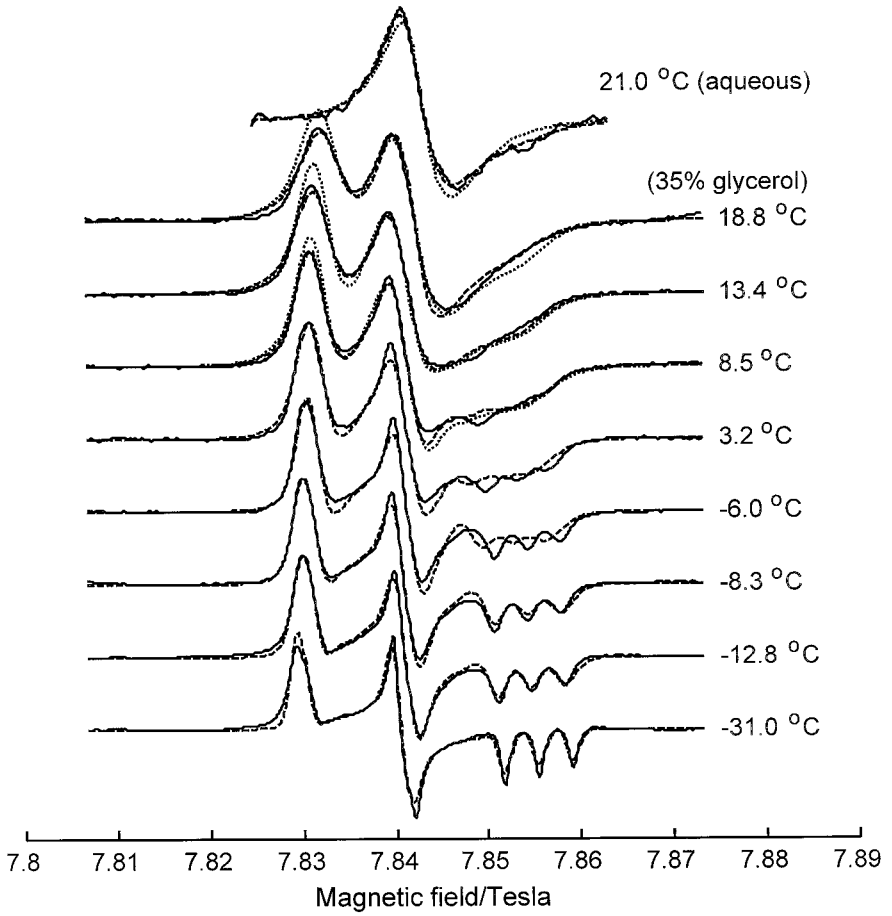

FIGURE 3 220 GHz EPR spectra of 700 μM spin-labeled pentamer TTC*TT in 50 mM HEPES buffer pH 7.4 at 21°C (*top spectrum*) and 3.9 mM pentamer in buffer with 35% (by volume) glycerol as a function of temperature. Dashed lines show the least-squares fits obtained for the FAR model as described in the text. Dotted lines for spectra at 21.0°C, 18.0°C, and 13.8°C show the spectrum calculated assuming an axially symmetric diffusion tensor as described in the text.

monomer in aqueous buffer at room temperature. The glycerol also served to prevent formation of ice crystals in the sample during temperature studies, and allowed measurement of the rigid limit spectrum from which the magnetic parameters of the label were obtained.

Slow-motional 220 GHz spectra were analyzed using the nonlinear least-squares program NLSL described by Budil et al. (1996). The temperature series for both the monomer and the pentamer were analyzed using a model of fully anisotropic rotation (FAR), assuming no local ordering of the probe, and taking the rotational diffusion axes to coincide with the magnetic tensor axes. Results from the nonlinear least-squares fits are given in Table 2, and the best-fit spectra are shown by the dashed lines in Figs. 2 and 3.

TABLE 1 Magnetic parameters of cytosine spin label

g_x[†]	2.00879
g_y[†]	2.00586
g_z[†]	2.00210
A_x/Gauss	5.5 ± 0.3
A_y/Gauss	5.8 ± 0.3
A_z/Gauss	37.0 ± 0.2

Determined by least-squares analysis of rigid limit 220 GHz spectrum of cytosine spin label.
[†]Estimated uncertainty in *g*-values is 5×10^5.

Several general observations can be made about the spectra in Figs. 2 and 3. The nitroxide parameters were determined from the near-rigid limit spectrum of the labeled pentamer and used for both species. Although the lowest-temperature spectrum from the monomer exhibits effects of residual motion on the microsecond time scale, the magnetic parameters of the nitroxide do not differ appreciably between the two species.

Interestingly, the g_x parameter, which is most sensitive to the polarity of the probe environment (Ondar et al., 1985; Earle et al., 1994) falls in a range corresponding to an effective "solvent" that is appreciably less polar than either pure water or water-glycerol mixtures (Ondar et al., 1985). The amount of inhomogeneous broadening in the g_x region is also noticeably less than that usually observed at high frequency from nitroxides in aqueous or highly polar environments (Earle et al., 1994). Similar effects have recently been observed for the g_x values of nitroxide-labeled proteins (Barnes et al., 1999). These observations suggest that the spin probe is shielded from the aqueous solvent to a significant degree, particularly in the pentamer for which data are available at a lower temperature.

The relatively small degree of inhomogeneous broadening is particularly interesting for the spin-labeled pentamer,

TABLE 2 Results from fits to slow-motional EPR spectra at 220 GHz using the full rotational anisotropy model

T/°C	$\Delta^{(0)}$*/G	$R_x^{\dagger}/s^{-1}$	$R_y^{\dagger}/s^{-1}$	$R_z^{\dagger}/s^{-1}$
		Monomer (75% glycerol)		
21	15.0	1.89×10^8	4.98×10^7	6.91×10^7
18.0	11.8	1.25×10^8	4.19×10^7	1.94×10^7
13.8	17.5	4.39×10^7	1.40×10^7	8.73×10^6
10.9	15.9	3.95×10^7	1.16×10^7	1.00×10^7
6.5	14.9	1.87×10^7	5.58×10^6	4.64×10^6
0.5	16.0	6.29×10^6	2.16×10^6	1.14×10^6
		Pentamer (60% glycerol)		
18.8	16.8	2.39×10^8	1.16×10^8	4.22×10^7
13.4	12.6	1.77×10^8	6.64×10^7	3.78×10^7
8.5	12.6	1.50×10^8	5.19×10^7	3.18×10^7
3.2	4.7	1.36×10^8	4.51×10^7	2.75×10^7
−6.0	4.7	7.48×10^7	2.52×10^7	1.62×10^7
−8.3	15.1	2.45×10^7	8.81×10^6	1.18×10^7
−12.8	14.5	1.62×10^7	7.60×10^6	6.78×10^6
−31.0	12.6	1.37×10^6	8.36×10^6	3.63×10^6

*$\Delta^{(0)}$ is orientation-independent Gaussian inhomogeneous broadening.
†Estimated uncertainty in R values is ±7% unless otherwise stated.

since the magnetic parameters of the nitroxide should in principle reflect the influence of the negatively charged phosphates of the DNA backbone in this case. Charged groups in fixed positions relative to the N—O bond do produce predictable changes in the ^{14}N hyperfine interaction (Swartz et al., 1997), which should also be reflected in the electronic g-factor. According to the treatment of Swartz et al. (1997) the observed shift in the g_x value corresponds to an average N—O bond orientation in which the oxygen is closest to the negative charges. However, if the backbone charges do influence the g_x value, the lack of significant broadening in the g_x peak would then suggest that the spatial distribution of the charges is relatively homogeneous, which seems unlikely.

The most prominent feature of the slow-motional spectra for both the monomer and pentamer is the well-resolved low-field ("x") peak, which remains close to its rigid-limit position over the entire temperature range. In contrast, the high-field "z" peaks broaden significantly and shift toward the center of the spectrum as the temperature increases, eventually merging with the central "y" peak. The y peak also broadens and shifts away from its rigid-limit value. This behavior is qualitatively consistent with preferred rotation about the x axis as predicted from the fast-motional linewidths.

As can be seen from the calculated spectra shown in Fig. 2, the FAR model provides a good fit to the spectra of the labeled monomer over the entire temperature range studied. More significantly, least-squares analysis permits resolution of all three elements of the rotational diffusion tensor in the slow-motional regime, despite the fact that R_y and R_z are relatively close in value. Spectra calculated with an axial diffusion tensor such that $R_{\parallel} = R_x$ and $R_{\perp} = (R_y R_z)^{1/2}$ deviated from the best-fit spectra calculated with $R_y \neq R_z$. The deviation was most noticeable at the higher temperatures within the slow-motional range. Spectra calculated with the assumption of axial symmetry are shown with dotted lines for the temperatures 18.0°C, 13.8°C, and 10.9°C in Fig. 2, and for the temperatures 21.0°C, 18.8°C, 13.4°C in Fig. 3. At lower temperatures, although the FAR model gave marginally better fits to the data (i.e., slightly smaller χ^2 values) than the axial rotation model, the improvement is not significant and it becomes impossible to distinguish the full anisotropy reliably. This is because the spectra become much less sensitive to rotation around all three probe axes as the motion approaches the rigid limit. However, the results from the FAR model gave reasonably consistent anisotropy parameters $\rho_x = 4.6 \pm 1.3$ and $\rho_y = 1.5 \pm 0.5$ over the temperature range studied, which are quite comparable to the anisotropy parameters obtained from the fast-motional linewidths. This result suggests that the overall rotation in glycerol solution is similar to that in water for both the monomer and the pentamer throughout the temperature range studied.

The capability of measuring the full anisotropy of labeled base motions has significant implications for the analysis of local base dynamics in DNA. Most importantly, it removes the assumption of an axial diffusion tensor that is inherent in the models presently used to analyze base motions. The additional anisotropy information thus provides an important additional means of discriminating effects of DNA base motions from motions of the spin probe itself.

In contrast to the results from the monomer label, spectra from the labeled pentamer could not be fitted over the entire temperature range using the FAR model. Although reasonable agreement could be achieved at the highest and lowest temperatures in the series, where the slow-motional lineshape is relatively less sensitive to the details of the motion,

there is noticeable deviation between the calculated and experimental results in the temperature range 8.0° to −6.0°C. The differences occur mainly near the z-peaks (cf. Fig. 3) with the z-peaks in the experimental spectrum remaining relatively sharp and well-resolved even as they shift toward the center at higher temperature. These features cannot be accounted for simply by adjusting rotational diffusion rates: motional rates high enough to cause the observed shift in the z-peaks also produce significantly broader lines than are observed.

An alternative model that may account for the features just noted is the microscopic order macroscopic disorder (MOMD) model introduced by Freed and co-workers (Meirovitch et al., 1984). This model assumes that the label is influenced by an orienting potential that produces microscopic ordering of the molecule relative to a local director axis that is fixed with respect to the macromolecule and is randomly oriented. If the motion of the macromolecule bearing the label is sufficiently slow on the 220 GHz EPR time scale, its motion can be treated as being essentially in the rigid limit, and the spectrum may be calculated by summing over the static distribution of local director orientations. Thus, the shift of the z-peaks could result from local ordering of the probe, since the spin-label would diffuse only within a limited range of orientations, thus limiting the degree to which the motion averages the spectral lineshape. The sharpness of the z-peaks may also reflect relatively lower rates of rotational diffusion in the "cage" surrounding the label.

Fig. 4 shows least-squares fittings to the three spectra from the labeled pentamer in the middle of the temperature range shown in Fig. 3 using a simplified MOMD model. The parameters determined from the fits are given in Table 3. To reduce the number of parameters needed, both the rotational diffusion tensor and the orienting potential were restricted to axial symmetry. The probe ordering potential represented using only the lowest-order term in the generalized spherical harmonic expansion of the potential function U:

$$U(\theta) = \frac{c_0^2}{2}(3\cos^2\theta - 1) \tag{2}$$

where θ is the angle between the z axis of the diffusion tensor and the local director and c^2_0 is an adjustable parameter expressed in units of kT. A diffusion tilt angle $\beta_d = \pi/2$ was introduced so that the diffusion z axis coincides with the magnetic x axis (i.e., the direction of the N—O bond).

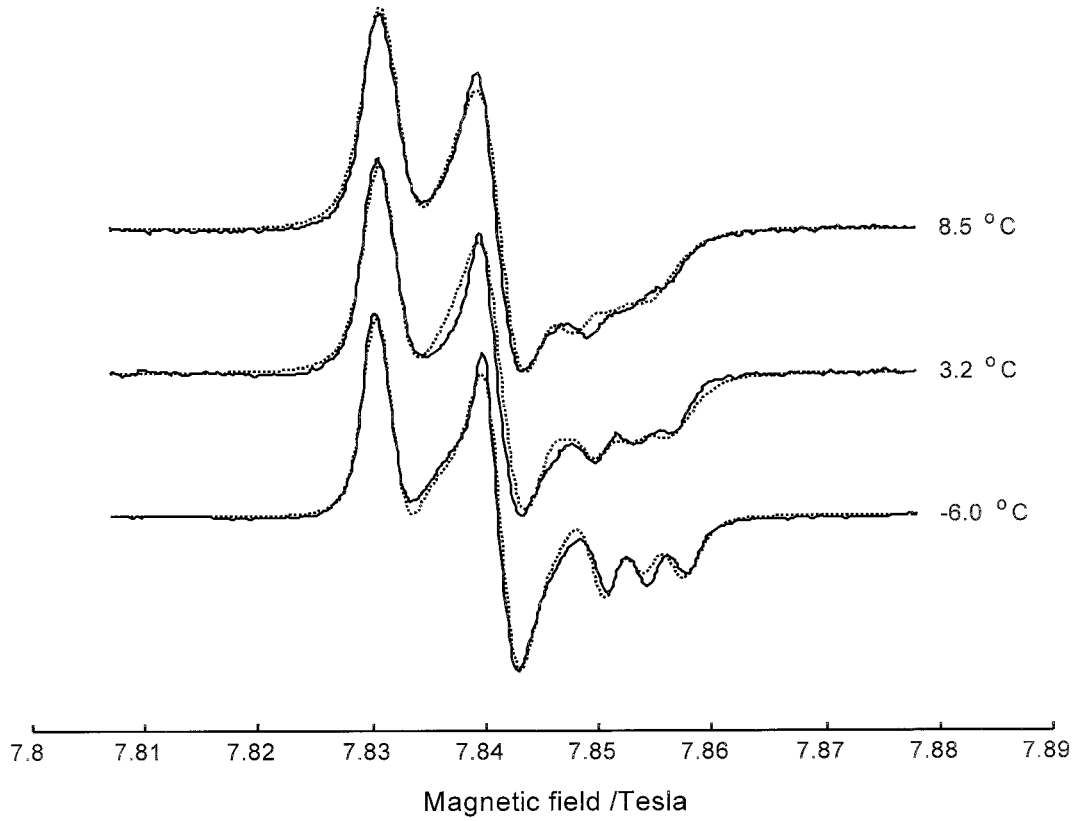

FIGURE 4 220 GHz EPR spectra of 3.9 mM spin-labeled pentamer TTC*TT in buffer: 35% glycerol at three temperatures in the middle of the range shown in Fig. 3. Dashed lines show the least-squares fits obtained for the MOMD model as described in the text. Dotted lines for spectra at 21.0°C, 18.8°C, 13.4°C, and 8.5°C show the spectrum calculated assuming an axially symmetric diffusion tensor as described in the text.

TABLE 3 Results from fits to slow-motional EPR spectra of spin-labeled pentamer at 220 GHz using the microscopic order, macroscopic disorder model

T/°C	$\Delta^{(0)}$*/G	$\Delta^{(2)}$*/G	$R_\perp{}^\dagger/s^{-1}$	$R_\parallel{}^\dagger/s^{-1}$	$c0^2/kT$	S
8.5	19.1	−15.1	6.16×10^7	1.60×10^8	2.95 ± 0.2	0.60 ± 0.04
3.2	17.7	−10.5	5.09×10^7	1.32×10^8	3.29 ± 0.2	0.64 ± 0.04
−6.0	18.7	−3.4	2.04×10^7	3.82×10^7	3.79 ± 0.2	0.69 ± 0.04

*Orientation-dependent Gaussian inhomogeneous broadening is $\Delta^{(0)} + \Delta^{(2)}\sin^2\psi$ where ψ is the local director tilt angle in the MOMD model.
†Estimated uncertainty in R values is ±7% unless otherwise stated.

The results of the FAR model were used as the starting parameters for the MOMD fits, taking $R_\parallel = R_x$ and $R_\perp = (R_yR_z)^{1/2}$. The rotational rates obtained using the MOMD model remained quite close to those obtained from the fully anisotropic rotation model. Thus, the improvements in the fits are mainly due to the increase of local ordering.

While the lineshapes calculated using this simplified MOMD model still deviate somewhat from the experimental data, they lead to appreciably lower χ^2 values than the FAR model fits shown in Fig. 3. More importantly, they reproduce the qualitative behavior noted above for the z-peaks of the spectrum. The agreement with experiment might be improved by additional parameters in the least-squares minimization that reflect greater detail of the motion, for example 1) a fully anisotropic rotational diffusion tensor, 2) higher-order nonaxial terms in the orienting potential, and 3) "diffusion tilt" between the magnetic and motional axes of the label. Nevertheless, the improvement afforded by even this simple MOMD model provides good evidence for local ordering effects in the oligomer that are not observed in the spin-labeled monomer.

One unusual feature of the MOMD results shown in Table 3 is the rather high local ordering that is needed to reproduce the features of the experimental spectra. Keyes and Bobst (1995) find order parameters in the range $S = 0.3–0.4$ for two-atom flexible tethers bound to double-stranded DNA. One might expect higher ordering in a double-stranded species resulting from a greater restriction of the label motion in the groove structure of the duplex in comparison with a single-stranded random-chain oligonucleotide. However, the analysis of the 220 GHz spectra using the MOMD model gives significantly higher order parameters in the range 0.6−0.7 as shown in Table 3. Such high ordering may be consistent with the finding that the magnetic parameters of the label reflect a largely nonpolar environment. In combination, these two observations suggest that the single-stranded pentamer could adopt a tightly packed micelle-like structure with the negatively charged phosphate groups on the periphery and the spin probe in close association with the hydrophobic bases at the center of the structure.

In the presence of local ordering, multifrequency spectroscopy and analysis will likely be needed to fully characterize the motions of the DNA and label over their wide dynamic ranges. The availability of a high frequency in addition to the standard 9 GHz in principle provides a direct means of resolving the effects of local probe dynamics from the influence of large-scale motions of the DNA. With slower motions "frozen out" at high frequency, one is able to measure the local ordering of the probe directly. At lower frequencies, where the probe motion falls into the fast-motion limit, the order parameters determined at high frequency may then be used to derive dynamically averaged tensors such as are presently used to model low-frequency data. The additional resolution at high field will allow measurement of higher-order terms in the potential, improving the accuracy of the effective tensors used for the lower-field studies.

It should be noted that the MOMD model will be strictly valid only when the motions of the probe and the labeled macromolecule occur on very different time scales. This condition enables the application of the rigid-limit approximation to the macromolecular motion at high EPR frequency, and the use of dynamically averaged effective tensors to represent the label motion at low EPR frequency. When both types of motion fall into the slow-motion region, or when the motions occur over a broad dynamic range, it becomes necessary to account for them explicitly. One elegant approach to solving this problem is the slowly relaxing local structure (SRLS) model treated by Polimeno and Freed (1995), which explicitly includes the rotational dynamics of the local structure that defines the orienting potential.

Given that a single-stranded pentamer produces slow-motional 220 GHz spectra in aqueous buffer near room temperature, larger DNA duplexes may be expected to exhibit overall dynamics approaching the rigid limit at this frequency. Thus, the range of EPR frequencies from 150 to 300 GHz appears to be nearly optimal for separating the effects of local probe motions from those of global bending and tumbling in spin-labeled DNA near physiological conditions.

CONCLUSION

The dynamics of a newly synthesized cytosine spin-label and the spin-labeled pentamer TTC*TT have been observed by quasioptical 220 GHz EPR in aqueous solution and at ambient temperature. Sufficient concentration sensitivity

has been achieved at this frequency to enable the 220 GHz spectrum to be measured using only nanomole amounts of labeled material.

The 220 GHz spectra exhibit great sensitivity to the dynamics of the label in the slow-motional regime, which was achieved for these relatively small molecules by adjusting the viscosity of the medium with glycerol. Specifically, the rotational rates around all three molecular axes of the label could be measured independently for the monomer species. The high-field spectra also revealed the presence of local ordering in the single-strand labeled pentamer, suggesting a micelle-like structure in which the label is tightly packed with the hydrophobic bases.

These preliminary results illustrate the appreciable amount of new information that is available about local base motions in DNA from high-field spin-label studies, and demonstrate the utility of multifrequency studies for accurately discriminating the effects of local versus global motions in labeled macromolecules.

We gratefully acknowledge Robert Rieger for assistance with the mass spectroscopy data.

This work was supported by funds to D.E.B. from the National Science Foundation (MCB 9600940) and to P.R.S. from the National Institutes of Health (5R01 CA72702-02).

REFERENCES

Altenbach, C., and W. L. Hubbell. 1994. Site-directed spin labeling of membrane proteins. *In* Membrane Protein Structure. S. H. White, editor. Oxford University Press, New York. 224.

Barnes, J. P., and J. H. Freed. 1997. Aqueous sample holders for high-frequency electron spin resonance. *Rev. Sci. Instrum.* 68:2838–2846.

Barnes, J. P., Z. Liang, H. S. Mchaourab, J. H. Freed, and W. L. Hubbell, 1999. Multifrequency electron spin resonance study of T4 lysozyme dynamics, *Biophys. J.* 76:3298–3306.

Berliner, L. J., and J. Reuben. 1989. Biological Magnetic Resonance, Vol. 8: Spin Labeling Theory and Applications, Plenum Press, New York.

Bobst, E. V., R. S. Keyes, Y. Y. Cao, and A. M. Bobst. 1996. Spectroscopic probe for the detection of local DNA bending at an AAA triplet. *Biochemistry.* 35:9309–9313.

Budil, D. E., K. A. Earle, and J. H. Freed. 1993. Full determination of the rotational diffusion tensor by electron paramagnetic resonance at 250 GHz. *J. Phys. Chem.* 97:1294–1303.

Budil, D. E., S. Lee, S. Saxena, and J. H. Freed. 1996. Nonlinear least-squares analysis of slow-motional EPR spectra in one and two dimensions using a modified Levenberg-Marquardt algorithm. *J. Magn. Reson. A.* 120:55–189.

Cardin, J. T., J. R Anderson, S. V. Kolaczkowski, and D. E. Budil. 1999. Quasioptical design for an EPR spectrometer based on a horizontal bore superconducting solenoid. *Appl. Magn. Reson.* 16273–16292.

Earle, K. A, J. K. Moscicki, M. Ge, D. E. Budil, and J. H. Freed. 1994. 250 GHz electron spin resonance studies of polarity gradients along the aliphatic chains in phospholipid membranes. *Biophys. J.* 66:1213–1221.

Froehler, B. C., S. Wadwani, T. J. Terhorst, and S. R. Gerrard. 1992. Oligodeoxynucleotide containing C-5 propyne analogs of 2′-deoxyuridine and 2′-deoxycytidine. *Tetrahedron Lett.* 33:5307–5310.

Hustedt, E. J., J. J. Kirchner, A. Spaltenstein, P. B. Hopkins, and B. H. Robinson. 1995. Monitoring DNA dynamics using spin-labels with different independent mobilities. *Biochemistry.* 34:4369–4375.

Hustedt, E. J., A. Spaltenstein, J. J. Kirchner, P. Hopkins, and B. H. Robinson. 1993. Motions of short DNA duplexes: an analysis of DNA dynamics using an EPR-active probe. *Biochemistry.* 23:1774–1787.

Kao, S. C., and A. M. Bobst. 1985. Local base dynamics and local structural features in RNA and DNA duplexes. *Biochemistry.* 24: 5465–5469.

Keyes, R. S., and A. M. Bobst. 1995. Detection of internal and overall dynamics of a two-atom-tethered spin-labeled DNA. *Biochemistry.* 34: 9265–9276.

Keyes, R. S., E. V. Bobst, and A. M. Bobst. 1997. Overall and internal dynamics of DNA as monitored by five-atom-tethered spin labels. *Biophys. J.* 72:282–290.

Kowert, B. 1981. Determination of the anisotropic and nonsecular contributions to ESR linewidths in liquids. *J. Chem. Phys.* 85:229–235.

Likhtenshtein, G. I. 1993. Biophysical Labeling Methods in Molecular Biology. Cambridge University Press, New York.

Meirovitch, E. A. Nayeem, and J. H. Freed. 1984. Analysis of protein-lipid interactions based on model simulations of electron spin resonance spectra. *J. Chem. Phys.* 88:3454–3465.

Millhauser, G. L. 1992. Selective placement of electron spin resonance spin labels: new structural methods for peptides and proteins. *Trends Biochem. Sci.* 17:448–452.

Ondar, M. A., O. Y. Grinberg, A. A. Dubinskii, and Y. A. Lebedev. 1985. Study of the effect of the medium on the magnetic-resonance parameters of nitroxyl radicals by high-resolution EPR spectroscopy. *Sov. J. Chem. Phys.* 3:781–792.

Pauly, G. T., I. E. Thomas, and A. M. Bobst. 1987. Base dynamics of nitroxide-labeled thymidine analogues incorporated into $(dA\text{-}dT)_n$ by DNA polymerase I from *Escherichia coli. Biochemistry.* 26:7304–7310.

Polimeno, A., and J. H. Freed. 1995. Slow motional ESR in complex fluids: the slowly relaxing local structure model of solvent cage effects. *J. Phys. Chem.* 99:10995–11006.

Reese, C. B., and P. A. Skone. 1984. The protection of thymine and guanine residues in oligodeoxribonucleotide synthesis. *J. Chem. Soc. Perkins. Trans. I.* 1263–1271.

Spaltenstein, A., B. H. Robinson, and P. B. Hopkins. 1988. A rigid and nonperturbing probe for duplex DNA motion. *J. Am. Chem. Soc.* 110: 1299–1301.

Spaltenstein, A., B. H. Robinson, and P. B. Hopkins. 1989. Sequence- and structure-dependent DNA base dynamics: synthesis, structure, and dynamics of site and sequence specifically spin-labeled DNA. *Biochemistry.* 28:9484–9495.

Strobel, O. K., R. S. Keyes, and A. M. Bobst. 1990. Base dynamics of local Z-DNA conformations as detected by electron paramagnetic resonance with spin-labeled deoxycytidine analogues. *Biochemistry*. 29: 8522–8528.

Swartz, R. N., M. Peric, S. A. Smith, and B. L. Bales. 1997. Simple test of the effect of an electric field on the ^{14}N-hyperfine coupling constant in nitroxide spin probes. *J. Phys. Chem. B* 101:8735–8739.